FULL PAPER

Dalton
www.rsc.org/dalton

Ag(I) complexes with alkylidene-bis(2-aminopyrimidines) as building units for discrete metallomacrocyclic frames. A structural and solution study†

Angel García-Raso,*[a] Juan J. Fiol,[a] Andrés Tasada,[a] Francisca M. Albertí,[a] Elies Molins,[b] Manuel G. Basallote,[c] María A. Máñez,[c] María J. Fernández-Trujillo[c] and David Sánchez[c]

[a] *Departament de Química, Universitat de les Illes Balears, Campus UIB, 07122, Palma de Mallorca, Spain*

[b] *Institut de Ciència de Materials de Barcelona (CSIC), Campus de la Autònoma, 08193, Cerdanyola, Spain*

[c] *Departamento de Ciencia de los Materiales e Ingeniería Metalúrgica y Química Inorgánica, Universidad de Cádiz, Apdo. 40, Puerto Real, 11510, Cádiz, Spain*

Received 14th June 2005, Accepted 29th July 2005
First published as an Advance Article on the web 30th August 2005

Alkylidene-bis(2-aminopyrimidines) (pyr_2C_x, $x = 2$–5) are useful ligands to interact with Ag(I) yielding discrete metallocycles. Crystal structures of the $[(pyr_2C_2)Ag(NO_3)]_2$ and $[(H\text{-}pyr_2C_4)Ag(NO_3)_2]_2$ have been isolated where each macrocyclic moiety interacts with their surroundings through weak interactions, yielding 3D discrete structures, On the other hand, the solution study shows that the equilibrium constants for the formation of $Ag(pyr_2C_x)^+$ complexes are higher than the literature values for Ag(I) complexes with single pyrimidines, although the differences could be explained by invoking the solid-state structures of the Ag(I)–pyr_2C_x complexes.

Introduction

The control of the self-assembly process between labile metal ions and flexible multidentate ligands is a key objective in the development of supramolecular coordination chemistry.[1] Obviously, this process is related with a variety of factors as the number, type and spatial disposition of the binding sites of ligands, the stereoelectronic preferences of metal ions, the solvent, the nature of counter ions, *etc.* The combination of all of this factors leads to numerous metallosupramolecular complexes with various structural topologies.[2]

Ag(I) is an interesting metal because several coordination geometries have been described, such as linear, T-shaped, trigonal, distorted tetrahedral, or octahedral,[3] each particular geometry being usually a consequence of the coordination properties of the ligands. In this context, pyrimidine and its derivatives are bidentate N,N-donor linking ligands with an interesting angular geometry that allows the building of multidimensional architectures,[4] such as discrete macrocyclic metal complexes or coordination polymers with open networks.[5] For this reason, we have prepared polymethylene-bis(2-aminopyrimidines) by a modification of a previously described methodology[6] and studied the capability of this type of ligands to yield Ag(I) complexes with interesting supramolecular structures.

Thus, in the present paper, we report the synthesis of several *N*,*N*′-bis(2-pyrimidyl)-α,ω-polymethylenediamines (pyr_2C_x, $x =$ 2–6) as building-blocks to prepare Ag(I)–supramolecular structures (Scheme 1). Different Ag(I)–pyr_2C_x complexes ($x = 2$ to 4) have been obtained and two of them, $[Ag(pyr_2C_2)(NO_3)]_2$ **1** and $[Ag(Hpyr_2C_4)(NO_3)_2]_2$ **4**, have been structurally characterised by X-ray diffraction. Moreover, solution studies of these compounds [equilibrium constants for the protonation of these ligands and for the formation of Ag(I) complexes] have been performed to achieve a better understanding of their chemistry. Our results show that these compounds form discrete inorganic Ag(I) metallocycles.

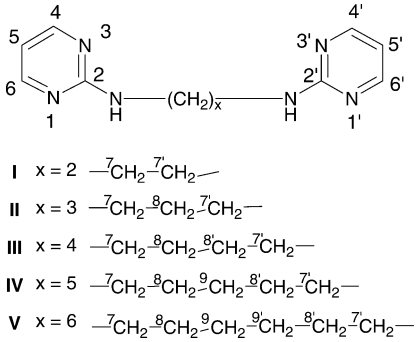

Scheme 1

Results and discussion

Description of the ligands

Crystal structures of three pyr_2C_x ligands have been solved by X-ray diffraction. These structures include the diprotonated forms of pyr_2C_2 **Ia** (Fig. 1), pyr_2C_4 **IIIa** (Fig. 2) and the neutral form of pyr_2C_5 **IV** (Fig. 3). Although no interactions between

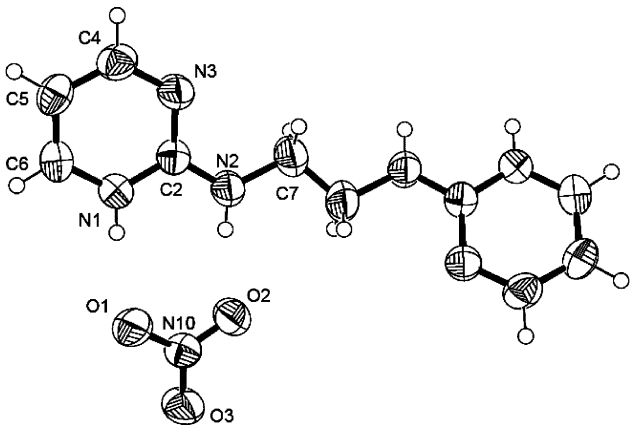

Fig. 1 ORTEP of $[(H\text{-}pyr)_2C_2](NO_3)_2$ **Ia** (second nitrate group has been omitted for clarity).

† Electronic supplementary information (ESI) available: Spectroscopic data of the ligands and complexes. Colour versions of Fig. 1–9. See http://dx.doi.org/10.1039/b508260a

DOI: 10.1039/b508260a

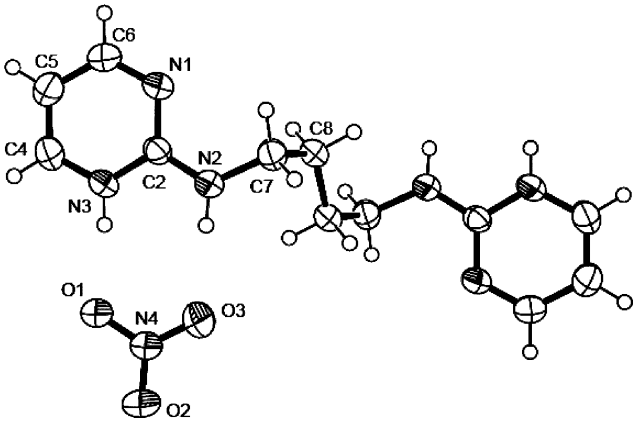

Fig. 2 ORTEP of $[(H\text{-}pyr)_2C_4](NO_3)_2$ **IIIa** (second nitrate group has been omitted for clarity).

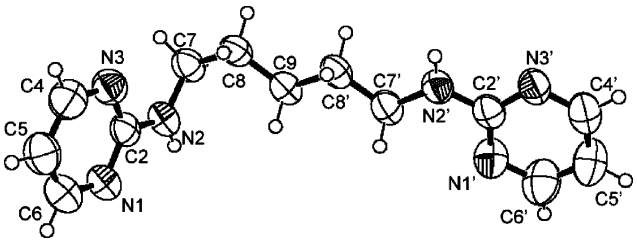

Fig. 3 ORTEP of pyr_2C_5 **IV**.

the two pyrimidine moieties of the same ligand are present in any of these three compounds, the conformation between them depends on the length of the polyalkylidene linker. Thus, based on the relationship between the relative disposition of the two pyrimidine-NH moieties (Fig. 4), diprotonated pyr_2C_2 **Ia** shows an *anti* conformation with a torsion angle of approximately 30° between the two rings, while the corresponding diprotonated pyr_2C_4 **IIIa** yields also an *anti* conformation with a non-coplanar disposition where the two pyrimidine rings are parallel [N(1)–C(2)–C(2′)–N(1′) 180°]. On the other hand, neutral pyr_2C_5 **IV** shows a nearly *anti* orthogonal conformation [N(1)–C(2)–C(2′)–N(1′) 108°]. Whereas neutral pyrimidines show symmetrical bond distances and angles, the corresponding protonated rings have bond distances and angles asymmetrically distributed, the larger C–C distance (*ca.* 1.39 Å) corresponding to the bond placed in the neighbourhood of the non-protonated pyrimidine nitrogen. An abnormal bond length between C(7)–C(7#) in pyr_2C_2 **Ia** [1.407(6) Å] should be mentioned. This is a nice example of the bicycle-pedalling vibration mode because the restricted movement of the N(2) atom related to its hydrogen bond with the O(2) atom of the nitrate group. This mode is often encountered in single bonded chains or macrocycles. In extreme cases gives rise to apparent or even real disordered atom positions. In the current disposition, the coupled vibration of the C(7) atom with its counterpart through the binary axis is conformationally favoured, because allows thermal activation keeping bond distances virtually constant. The average bonding distance appears shorter in the same manner than in the bicycle analogy (the two legs are closer than the distance between pedals).

The crystal structure of the neutral pyr_2C_5 **IV** ligand is formed by means a tandem of intermolecular hydrogen bonds N(2)–H···N(1′#) and N(2′#)–H···N(1) [distance N···N 3.01 and 3.10 Å, angle N–H···N 167 and 175°, respectively] (Fig. 5) that yields sheets in a zigzag disposition, which are separated by approximately 3.9 Å among them. On the other hand, in the protonated ligands a similar tandem of hydrogen bonds is observed [pyr_2C_2: N(1)–H···O(1) and N(2)–H···O(2), distance N···O 2.85 and 2.79 Å, angle N–H···O 171 and 170°, respectively; pyr_2C_4: N(3)–H···O(1) and N(2)–H···O(3) distance N···O 2.72 and 2.92 Å, angle N–H···O 174 and 162°, respectively]. There are also some interactions between the protonated pyrimidine moieties and the nitrate groups through the existence of several weak C–H···O interactions [distance and bond angle C–H···O: for pyr_2C_2 C(4)/C(6)···O(3)(nitrate) at 3.27/3.30 Å and 146/157°; for pyr_2C_4 C(4)···O(1)(nitrate)/O(3)(nitrate) at 3.33/3.31 Å and 158/146°].[7]

Structural characterization of the Ag(I)–pyr_2C_x complexes

The results obtained from the equilibrium studies (see below) indicate that formation of Ag(I)–L complexes occurs even in acidic conditions, although an excess of Ag(I) must be used to favour the complete formation of metal complexes (see Experimental section). By working under these conditions, solid samples were isolated. However, the unequivocal identification of the Ag(I) complexes by means of usual spectroscopic techniques (IR and ^1H and ^{13}C NMR) is very difficult because their spectra are very similar to the ligands (see Table 1). In our hands, the rapid characterisation of the complexes have been made according to (i) appearance of a broad intense band, corresponding to the N–O asymmetric stretching mode, $\nu(NO_3^-)$, at around

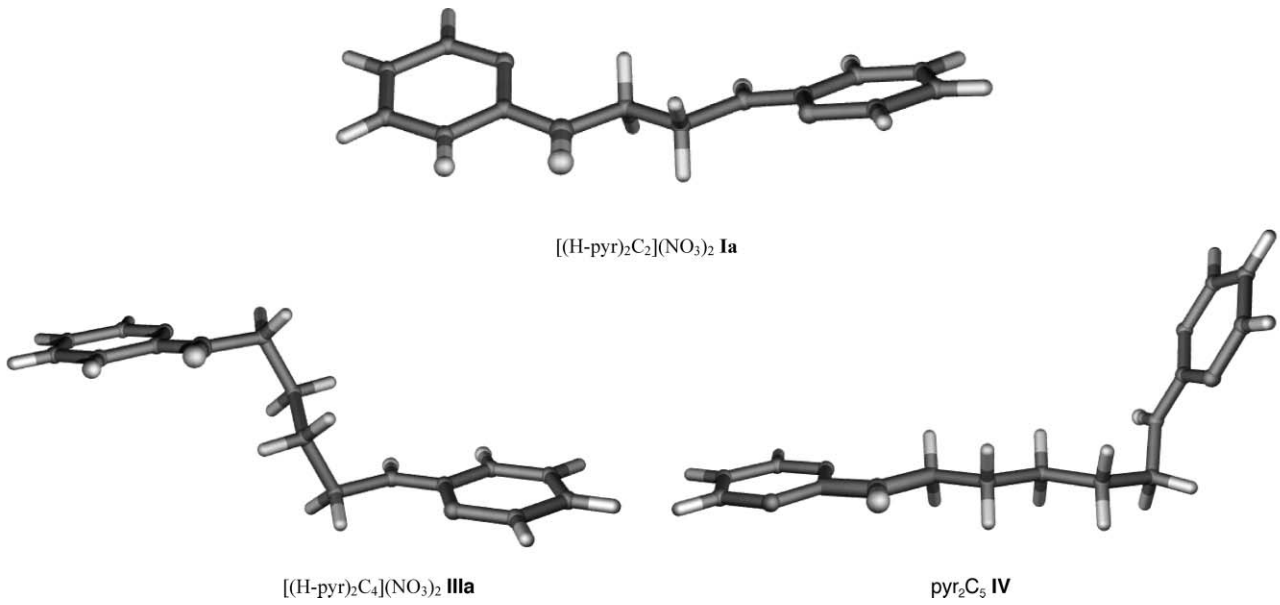

Fig. 4 Effect of the linker length on the relative conformations of the two pyrimidine moieties in the three ligands.

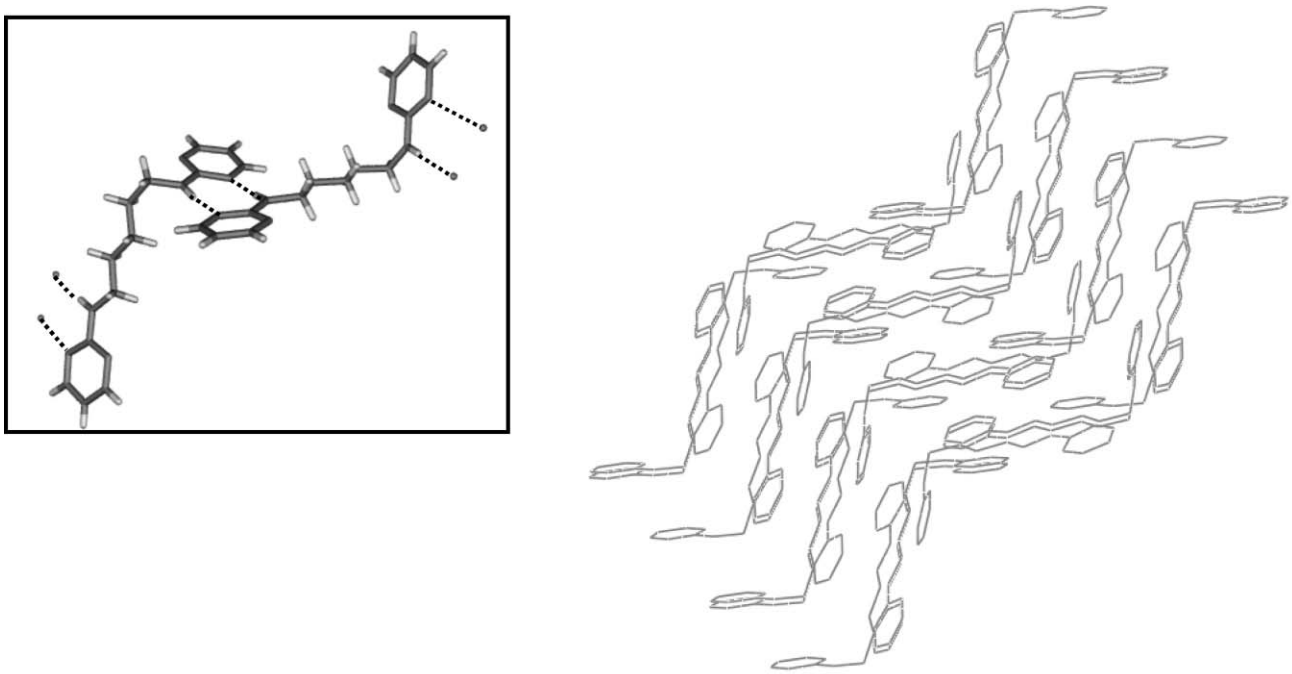

Fig. 5 Crystal packing of pyr_2C_5 **IV**.

1380 cm^{-1},[3] which is in agreement with the presence of nitrate in the structure (the IR spectrum only would show nitrate band in the complexes or in the protonated ligands) and (ii) thermal gravimetric analysis, which shows the ligand : Ag(I) ratio present in each structure.

In the pyr_2C_2–Ag complex **1**, the crystal structure is formed by distorted $L_2Ag_2^{2+}$ 18-membered-macrocyclic units with two nitrate groups placed at the top and bottom of each cyclic unit: the $NO_3[O(2)] \cdots [O(2)]O_3N$ distance is 3.44 Å and the $Ag \cdots Ag$ distance is 6.63 Å (Fig. 6). Moreover, the four NH groups adopt a *syn* disposition directed to the centre of the macrocyclic structure [$NH \cdots NH$ distances: $N(2) \cdots N(2\#)$, 5.83 Å and $N(2') \cdots N(2'\#)$, 6.43 Å]. The two pyrimidine moieties corresponding to a single ligand show a nearly orthogonal geometry [torsion angle between rings, 107°] and the opposite rings of each macrocycle are parallel. The Ag(I) ions show a quasi-linear coordination to two pyrimidine moieties of two different ligands [N(1)–Ag(1) 2.170(2) and N(1′)–Ag(1) 2.1804(19) Å; N(1)–Ag(1)–N(1′) 170.08(8)°] (Table 2). Three ancillary weaker bonds can be considered to complete the coordination sphere: two nitrate groups [Ag(1)–O(1) 2.64 Å and $Ag(1) \cdots O(1\#)$ 2.74 Å] and a pyrimidine ligand from other cyclic structure [Ag(1)–N 3.128 Å]. The different macrocyclic structures interact *via* a tandem of two $Ag \cdots O(nitrate)$ groups [$(NO_3)[O(1)] \cdots Ag(1\#)$ and $(NO_3)[O(1\#)] \cdots Ag(1)$ at 2.74 Å]. The crystal structure is completed by means of stacking interactions between pyrimidine rings from different crystal units [$C(2) \cdots C(4\#)$ and $C(4) \cdots C(2\#)$ at 3.36 Å) and all these interactions determine a structure formed by layers which interact *via* stacking among them (Fig. 7).

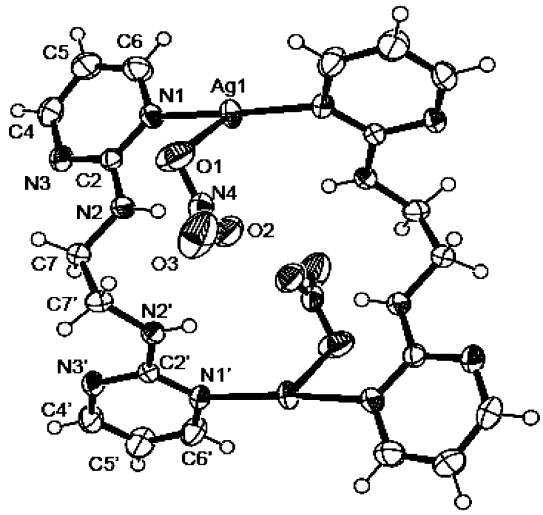

Fig. 6 ORTEP of dimeric Ag(I) complex with pyr_2C_2 (L) $[AgL(NO_3)]_2$ **1**.

Contrarily to the pyr_2C_2 complex, the corresponding Ag(I)-pyr_2C_4 complex **4** contains the ligand in a mono-protonated state (Fig. 8). The ligand arrangement in the complex shows a practically linear planar disposition where the two pyrimidine moieties of each ligand assume a completely different role: one neutral pyrimidine interacts directly with the Ag(I) ion and the other one is protonated and only interacts with the nitrate groups *via* H-bonds similar to those previously described for protonated ligands [$N(1')–H \cdots O(nitrate_1)$ and $N(2')–H \cdots O(nitrate_1)$, bond distances: 2.99 and 2.92 Å; angles: 156 and 163°, respectively] (Table 2). Moreover, an additional H-bond, $N(1')–H \cdots O(nitrate_2)$ must be considered (bond distance: 3.10 Å, angle: 130°). On the other hand, two neutral pyrimidine moieties corresponding to two different ligands interact directly with a Ag(I) ion yield a $(pyrimidine)_2Ag_2^{2+}$ cyclic structure that is repeated through the crystal. This $(pyrimidine)_2Ag_2^{2+}$ cyclic structure yields an eight-membered cycle with an $Ag \cdots Ag$ distance 5.67 Å, significantly smaller than for the Ag(I)-pyr_2C_2 complex. These two pyrimidine rings show a parallel disposition with a stacking between $N(1) \cdots C(2\#)$ and $C(2) \cdots N(1\#)$ at 3.32 Å. Each metal ion is nearly co-planar with one pyrimidine moiety and, because of the spacial disposition of the two pyrimidine rings in the metallocyclic unit previously described, the metallocycle is distorted and the bond between Ag(I) and the other pyrimidine ring is weaker. As a result, the Ag(I) coordination geometry corresponds to a very distorted tetrahedral disposition [bond angles between 140.76(11) and 73.74(11)°] with two pyrimidine groups [distances Ag–N(1) at 2.247(3) Å and Ag–N(3) at 2.634(3) Å] and two nitrate groups [distances Ag–O(1) at 2.393(3) Å and Ag–O(4) at 2.316(3) Å]. An additional H-bond interaction between one coordinated nitrate group and the exocyclic N–H must be mentioned [distance

Table 1 Selected IR and NMR data of the ligands

IR (ν_{max}/cm^{-1})		ν(NH)	ν(ring) + δ(NH)				$\nu_{asym}(NO_3)$
pyr_2C_2	**I**	3267s	1593vs, 1454s, 1538vs, 1421s, 1359s				—
$[(H\text{-}pyr)_2C_2](NO_3)_2$	**Ia**	—	1638vs br, 1567m, 1543m, 1353s				1384s, br
$pyr_2C_3{\cdot}2H_2O$	**II**	3261s	1597vs, 1535vs, 1454vs, 1416m, 1361s				—
pyr_2C_4	**III**	3257s	1599vs, 1542vs, 1463vs, 1416vs, 1369s				—
$[(H\text{-}pyr)_2C_4](NO_3)_2$	**IIIa**	3253m	1652vs, 1571m, 1615vs, 1329vs				1383vs
pyr_2C_5	**IV**	3264s	1594vs, 1538vs, 1457s, 1415 m, 1366s				—
pyr_2C_6	**V**	3268vs	1588vs, 1533vs, 1454vs, 1419vs, 1355s				—
NMR δ_H (DMSO-d_6)		H(4)/H(6)/H(4′)/H(6′)	N–H	H(5)/H(5′)	H(7)/H(7′)	H(8)/H(8′)	H(9)/H(9′)
pyr_2C_2	**I**	8.25 br d, J_{est} 4.8 Hz	7.17 br s	6.55 br t, J_{est} 4.8 Hz	3.43 br d	—	—
$[(H\text{-}pyr)_2C_2](NO_3)_2$	**Ia**	8.50 br d, J_{est} 5.1 Hz	—	6.85 br t	3.57 br s	—	—
$pyr_2C_3{\cdot}2H_2O$	**II**	8.24 d, J 4.8 Hz	7.13 br t	6.52 t, J 4.8 Hz	3,30 br q, J_{est} 6.6 Hz	br qui, J_{est} 6.6 Hz	—
pyr_2C_4	**III**	8.23 d, J 4.8 Hz	7.12 br t	6.51 t, J_{est} 4.8 Hz	3,25 m	1.54 br m	—
$[(H\text{-}pyr)_2C_4](NO_3)_2$	**IIIa**	8.55 d, J_{est} 5.1 Hz	—	6.88 t, J_{est} 5.1 Hz	3,38 br s	1.62 br s	—
pyr_2C_5	**IV**	8.23 br d, J_{est} 4.8 Hz	7.10 br t	6.51 br t, J_{est} 4.8 Hz	3.23 br q, J_{est} 6.9 Hz	1.52 br qui, J_{est} 6.9 Hz	1.34 m
pyr_2C_6	**V**	8.13 br d, J_{est} 4.8 Hz	7.00 br t	6.41 br t, J_{est} 4.8 Hz	3.11 br q	1.40 m	1.21 m
NMR δ_C (DMSO-d_6)		C(2)/C(2′)	C(4)/C(6)/C(4′)/C(6′)	C(5)/C(5′)	C(7)/C(7′)	C(8)/C(8′)	C(9)/C(9′)
pyr_2C_2	**I**	162.3	158.0	110.1	40.3	—	—
$[(H\text{-}pyr)_2C_2](NO_3)_2$	**Ia**	*ca* 160 br peak	157.0	110.5	40.4	—	—
$pyr_2C_3{\cdot}2H_2O$	**II**	162.3	157.9	109.8	38.3	28.8	—
pyr_2C_4	**III**	162.3	157.9	109.6	40.4	26.5	—
$[(H\text{-}pyr)_2C_4](NO_3)_2$	**IIIa**	157.1 br peak	156.2	109.5	40.6	25.6	—
pyr_2C_5	**IV**	162.3	157.8	110.5	40.5	28.7	24.0
pyr_2C_6	**V**	162.3	157.8	109.6	40.5	28.9	26.3
IR (ν_{max}/cm^{-1})		ν(NH)	ν(ring) + δ(NH)				$\nu_{asym}(NO_3)$
$[Ag(pyr_2C_2)(NO_3)]_2$	**1**	3302s	1597vs, 1572vs, 1531vs, 1460s, 1362s				1386s
$pyr_2C_3{\cdot}AgNO_3$[a]	**2**	3257m	1596s, 1540s, 1459m, 1353s				1382vs
$pyr_2C_4{\cdot}AgNO_3$[b]	**3**	3279s	1596vs, 1573vs, 1538vs, 1462vs, 1364vs				1384vs
$[Ag(H\text{-}pyr_2C_4)(NO_3)_2]_2$	**4**	3257s	1670s, 1600vs, 1579vs, 1543vs, 1464vs, 1346vs				1385vs
NMR δ_H (DMSO-d_6)		H(4)/H(6)/H(4′)/H(6′)	N–H	H(5)/H(5′)	H(7)/H(7′)	H(8)/H(8′)	H(9)/H(9′)
$[Ag(pyr_2C_2)(NO_3)]_2$	**1**	8.30 br d, J_{est} 4.8 Hz	7.30 br s	6.60 br t, J_{est} 4.8 Hz	3.46 br s	—	—
$pyr_2C_3{\cdot}AgNO_3$[a]	**2**	8.29 br d, J_{est} 4.8 Hz	7.24 br t	6.59 br t, J_{est} 4.8 Hz	3.33 br q	1.78 br quin J_{est} 6.9 Hz	—
$pyr_2C_4{\cdot}AgNO_3$[b]	**3**	8.27 d, J 4.8 Hz	7.20 t	6.56 t, J 4.8 Hz	3,28 br dt	1.56 br m	—
$[Ag(H\text{-}pyr_2C_4)(NO_3)_2]_2$[c]	**4**	8.39 br m	7.80 br s	6.70 br m	3,31 br s	1.58 br s	—
NMR δ_C (DMSO-d_6)		C(2)/C(2′)	C(4)/C(6)/C(4′)/C(6′)	C(5)/C(5′)	C(7)/C(7′)	C(8)/C(8′)	C(9)/C(9′)
$[Ag(pyr_2C_2)(NO_3)]_2$	**1**	161.8	158.5	110.1	40.2	—	—
$pyr_2C_3{\cdot}AgNO_3$[a]	**2**	161.8	158.5	109.9	38.5	28.6	—
$pyr_2C_4{\cdot}AgNO_3$[b]	**3**	162.4	158.8	110.2	40.9	26.9	—
$[Ag(H\text{-}pyr_2C_4)(NO_3)_2]_2$[c]	**4**	159.0	157.7	109.6	40.5	26.0	—

[a] Tentatively proposed as $[Ag(pyr_2C_3)(NO_3)]_2$. [b] Tentatively proposed as $[Ag(pyr_2C_4)(NO_3)]_2$. [c] The spectrum shows that the two pyrimidine rings are not completely equivalent.

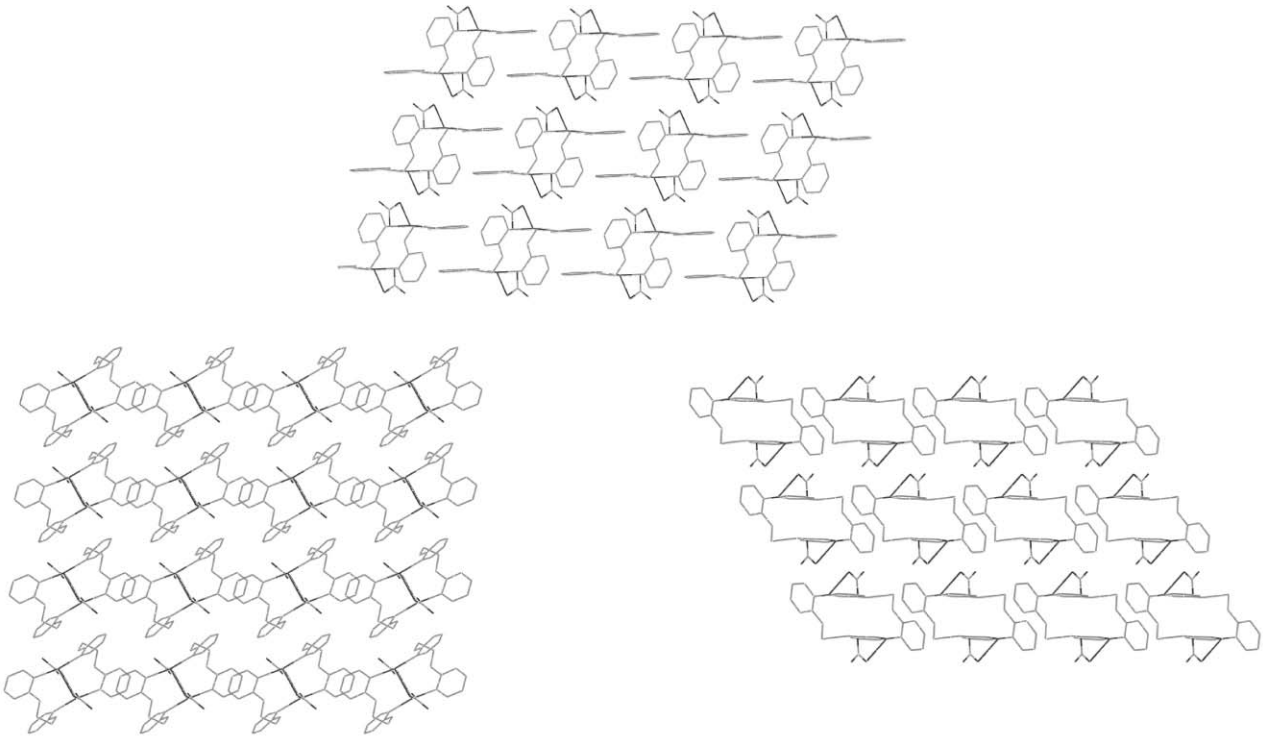

Fig. 7 Crystal packing of Pyr_2C_2–Ag complex **1** (views along *a*, *b*, *c* axis, respectively).

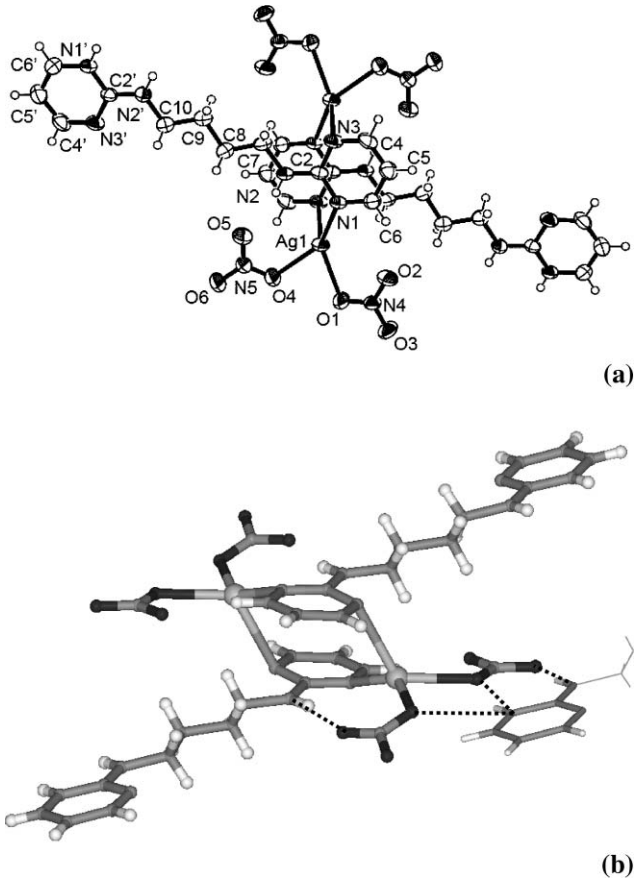

Fig. 8 (a) ORTEP of dimeric Ag(I) complex with protonated pyr_2C_4 (HL) $[Ag(HL)(NO_3)_2]_2$ **4**. (b) Ball-and-stick representation of the dimeric Ag(I)–protonated pyr_2C_4 complex **4** showing the additional ligand–nitrate interactions.

N(2)···O(5) 3.06 Å and angle N(2)–H···O(5), 167°]. The crystal structure is formed by dimers which interact among them by means of H-bonds forming different layers (Fig. 9).

Table 2 Selected lengths (Å) and bond angles (°) for complexes **1** and **4**

$Pyr_2C_2 \cdot AgNO_3$ **1**			
N(1)–Ag(1)	2.170(2)	Ag(1)–N(1)#	2.180(2)
C(6)–N(1)–Ag(1)	118.43(18)	C(6)#–N(1)#–Ag(1)	118.37(16)
C(2)–N(1)–Ag(1)	124.05(16)	C(2)#–N(1)#–Ag(1)	124.59(16)
N(1)–Ag(1)–N(1)#	170.08(8)		
H-$Pyr_2C_4 \cdot AgNO_3 \cdot HNO_3$ **4**			
Ag(1)–N(1)	2.247(3)	Ag(1)–N(3)#1	2.634(3)
Ag(1)–O(4)	2.316(3)	Ag(1)–O(1)	2.393(3)
N(3)–Ag(1)#1	2.634(3)		
N(1)–Ag(1)–N(3)#1	91.01(11)	O(4)–Ag(1)–O(1)	73.74(11)
N(1)–Ag(1)–O(4)	140.76(11)	O(4)–Ag(1)–N(3)#1	99.72(12)
N(1)–Ag(1)–O(1)	133.89(11)	O(1)–Ag(1)–N(3)#1	116.12(12)
C(2)–N(1)–Ag(1)	120.6(2)	C(2)–N(3)–Ag(1)#1	111.2(2)
C(6)–N(1)–Ag(1)	119.2(2)	C(4)–N(3)–Ag(1)#1	104.0(2)
N(5)–O(4)–Ag(1)	115.8(2)	N(4)–O(1)–Ag(1)	109.5(2)

Symmetry transformations used to generate equivalent atoms: #1 $2-x,1-y,1-z$ (in **1**), #1 $-x+1,-y,-z$ (in **4**).

Equilibrium studies on ligand protonation and Ag(I) complex formation

Despite the bioinorganic relevance of the interactions between metal ions and pyrimidine bases and the interesting structural aspects of the Ag(I)–pyrimidine complexes, the number of equilibrium studies on this kind of systems is still very limited.[8–10] For this reason, a potentiometric determination of the equilibrium constants for ligand protonation and formation of Ag(I) complexes was carried out for the pyr_2C_x molecules (Table 3). Two protonation constants were found for all the ligands, which indicates the existence of the equilibria shown in eqns (1) and (2) with log K_{H1} values in the range 3.75–4.33 and a log K_{H2} range of 1.93–2.96. Thus, in acidic solutions the ligands exist as a mixture of the H_2L^{2+}, HL^+ and L species (L = pyr_2C_x), the relative concentrations of them depending on the pH value and the

Table 3 Equilibrium data for protonation and formation of Ag(I) complexes with the pyr_2C_x ($x = 2$–5) ligands and the related pyrBu compound

Equilibrium	Constant[a]	Ligand				
		pyr_2C_2	pyr_2C_3	pyr_2C_4	pyr_2C_5	pyrBu
$L + H^+ = HL^+$	$\log K_{H1}$	3.75	4.01	4.33	4.20	3.92
$HL^+ + H^+ = H_2L^{2+}$	$\log K_{H2}$	1.93	2.78	2.96	2.75	—
$L + 2H^+ = H_2L^{2+}$	$\log \beta_{H2L}$	5.68	6.79	7.29	6.95	—
	$\log(K_{H1}/K_{H2})$	1.82	1.23	1.37	1.45	—
$L + Ag^+ = LAg^+$	$\log K_{Ag1}$	3.22	3.53	3.46	3.45	2.36
$LAg^+ + Ag^+ = LAg_2^{2+}$	$\log K_{Ag2}$	3.07	3.10	3.23	3.15	—
	$\log(K_{Ag1}/K_{Ag2})$	0.15	0.43	0.23	0.30	
$L + 2Ag^+ = LAg_2^{2+}$	$\log \beta_{LAg2}$	6.29	6.63	6.69	6.60	—
$L + Ag^+ + H^+ = HLAg^{2+}$	$\log \beta_{HLAg}$	—	7.13	7.20	7.48	—
$HL^+ + Ag^+ = HLAg^{2+}$	$\log K_{H-Ag}$	—	3.12	2.87	3.28	
$LAg^+ + H^+ = HLAg^{2+}$	$\log K_{Ag-H}$	—	3.60	3.74	4.03	

[a] The standard deviations in the $\log \beta$ values are in the 0.01–0.03 range for ligand protonation and 0.03–0.08 for complex formation.

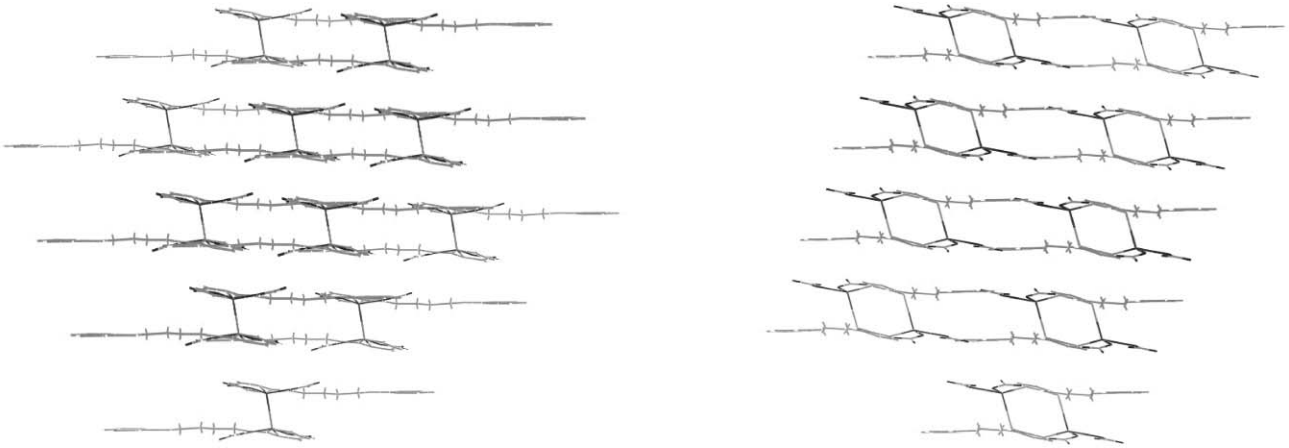

Fig. 9 Two different views of crystal packing in $[Ag(HL)(NO_3)_2]_2$ complex **4**.

nature of the ligand. This is illustrated in the species distribution curves included in Fig. 10 for the case of the pyr_2C_3 ligand (the curves for the other ligands show only minor differences). At pH higher than *ca.* 5.5, the ligand exists exclusively in the L form, whereas at lower pH significant amounts of HL^+ and H_2L^{2+} are formed. The maximum concentration of the mono-protonated HL^+ species is achieved at pH close to 3.3, but it never represents more than *ca.* 70% of the total ligand. Although the maximum relative amount of H_2L^{2+} is only 65% at pH 2.5 (the lowest pH value measured in the titrations), complete conversion of the ligand to this form will occur in more acidic solutions.

$$L + H^+ \rightleftharpoons HL^+; K_{H1} \quad (1)$$

$$HL^+ + H^+ \rightleftharpoons H_2L^{2+}; K_{H2} \quad (2)$$

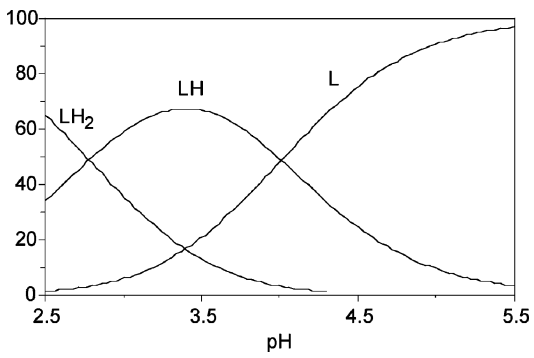

Fig. 10 Species distribution curves for the protonation of the pyr_2C_3 ligand ($C_L = 0.001$ M). Similar results are obtained with the other ligands.

All the $\log K_{H1}$ values for the pyr_2C_x ligands are close to the value of 3.92 found for the pyrBu ligand, which was studied for comparative purposes because it contains a single pyrimidine unit with a *n*-butyl group at the same position of the polymethylene chain in the pyr_2C_x ligands. The values are also very close to that reported for 2-aminopyrimidine (3.89),[8] which indicates that alkyl substitution at the N(2) position does not cause significant changes in the basicity of these compounds. However, it must be mentioned that all these values are significantly higher than that corresponding to free pyrimidine (2.45).[9]

Because the pyr_2C_x ligands contain two equivalent pyrimidine sub-units, it is also expected on the basis of statistical considerations that the equilibrium constant for the protonation of the first sub-unit be four times larger than that corresponding to protonation of the second pyrimidine, *i.e.* the statistical prediction for $\log(K_{H1}/K_{H2})$ is $\log 4 = 0.60$. However, the statistical considerations are only valid when both sub-units behave independently and so, significant deviations can be found in the presence of steric or electrostatic interactions between them. Because of the flexibility of the ligands, steric effects between the pyrimidine sub-units are not expected to be significant. Moreover, all the values of $\log(K_{H1}/K_{H2})$ are higher than 0.60 and indicate that protonation of a pyrimidine ring causes a significant electrostatic interaction with a second incoming proton, which leads to a decrease in the equilibrium constant for the protonation of the second ring, even for the ligands with larger spacers, [$\log(K_{H1}/K_{H2})$ is close to 1.3 (K_{H1}/K_{H2} close to 20)]. For the pyr_2C_2 ligand, the smaller size of the spacer leads to stronger electrostatic repulsions between the protonated sub-units and the decrease of the second protonation

constant is even more pronounced and far from the statistical prediction [$\log(K_{H1}/K_{H2}) = 1.82$; $K_{H1}/K_{H2} = 66$].

On the other hand, all the pyr_2C_x ligands with $x > 2$ form LAg^+, LAg_2^{2+} and $HLAg^{2+}$ complexes with similar values of the stability constants. For the case of pyr_2C_2, formation of the $HLAg^{2+}$ species was not detected in the analysis of the potentiometric curves, and the stability constant for the LAg^+ species is somewhat smaller than the values found for the other ligands. For the more general case of the pyr_2C_x ligands with $x > 2$, the stoichiometry of the complexes suggests that the pyrimidine sub-units of the ligands are able to accept either a proton or an Ag^+ ion and that all the possible combinations of two of these cations linked to a single molecule of pyr_2C_x exist, which leads to complex species distribution curves as those shown in Fig. 11. For a Ag(I) : L molar ratio of 1 : 1, none of the complexes represents more than 40% of the total ligand in the pH range covered in the potentiometric titrations. At the more acidic pH values, the species $HLAg^{2+}$ coexists with the protonated forms of the ligand, whereas at higher pH significant amounts of LAg^+ and LAg_2^{2+} are formed in equilibrium with L and HL^+. As expected, the amount of complexes formed increases significantly when the Ag(I) : L ratio is 2 : 1 (see Fig. 11(b)).

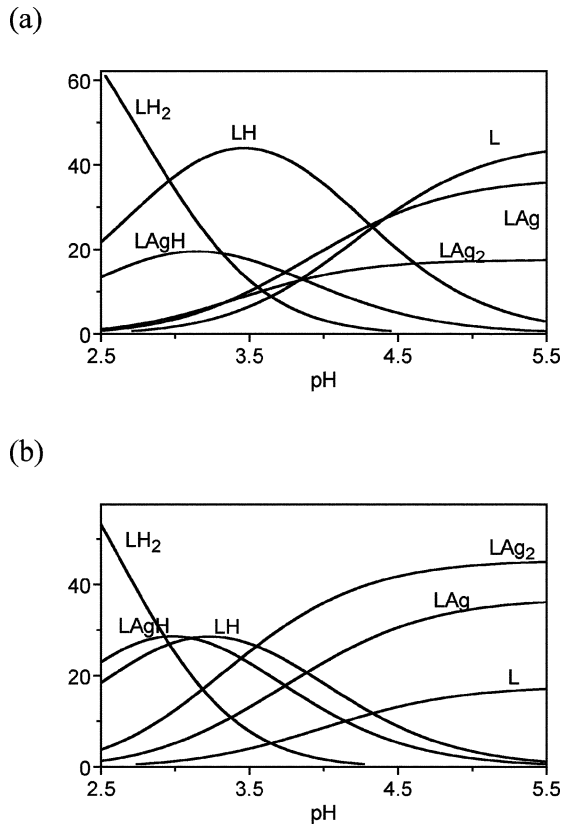

Fig. 11 Species distribution curves for the formation of Ag(I) complexes with pyr_2C_4: (a) 1 : 1 molar ratio ($C_{Ag} = C_L = 0.001$ M), (b) 2 : 1 molar ratio ($C_{Ag} = 2C_L = 0.002$ M).

The LAg^+ complexes of the pyr_2C_x ligands are more stable (one log unit) than the Ag(I)–pyrBu complex (see Table 3). In addition, the values of $\log K_{Ag1}$ in the range 3.22–3.53 indicate that the LAg^+ complexes have a stability higher than the analogous complexes with related ligands containing a single pyrimidine ring. Thus, $\log K_{LAg}$ for the complexes with pyrimidine, *N*-butylpyrimidine, 2-amino-1,3-diazine, 4-methyl-1,3-diazine and 2-amino-4-methyl-1,3-diazine are 1.61, 2.36, 2.27, 1.91 and 2.03, respectively.[8,10] Whereas the lower stability of the pyrimidine and 4-methyl-1,3-diazine complexes could be explained by the lower basicity of the ligands, the other compounds have a basicity similar to the pyr_2C_x derivatives and similar values of the stability constants for complex formation would be expected. The simplest interpretation for the high values of $\log K_{Ag1}$ for the pyr_2C_x complexes would be to consider that both pyrimidine sub-units participate in coordination to the Ag^+ ion in the LAg^+ species, but in that case the $\log K_{Ag-H}$ and $\log K_{Ag2}$ values for the addition of a proton or a second Ag^+ to the LAg^+ complexes should be smaller than the values in Table 3 as these processes would then involve de-coordination of one of the pyrimidine sub-units. A more reasonable explanation to the additional stabilisation observed for the Ag(I)–pyr_2C_x complexes can be made from a comparison of the crystal structures of the $[Ag(pyr_2C_2)(NO_3)]_2$ **1** and $[Ag(Hpyr_2C_4)(NO_3)_2]_2$ **4** complexes previously described with that reported[11] for [Ag(2-aminopyrimidine)$_2$](CF_3SO_3)·0.5H_2O. Whereas the structure of the latter complex reveals a linear coordination environment around the Ag(I) ion in which both 2-aminopyrimidine ligands act as monodentate ligands coordinated through one endocyclic nitrogen N(1), the structures of the pyr_2C_x complexes yield dimeric metallomacrocycles. If these structures are maintained in solution, they would explain the high stability of the complexes derived from the potentiometric data. Additional evidence favouring this interpretation is provided by the fact that the log β values for the formation of AgL_2^+ complexes with two equivalent molecules containing a single pyrimidine unit are 2.98 (pyrimidine), 3.67 (2-amino-4-methyl-1,3-diazine) and 3.24 (4-methyl-1,3-diazine),[8,10] all of them quite close to the values of $\log K_{Ag1}$ for the pyr_2C_x ligands in Table 3.

On the other hand, for the pyr_2C_x ligands the Ag^+–L interactions are less stable than the H^+–L interactions, as revealed by the fact that the $\log K_{Ag1}$ values are 0.48–0.87 units smaller than the corresponding $\log K_{H1}$ values. In contrast, the $\log K_{Ag2}$ values are 0.27–0.40 units higher than $\log K_{H2}$ for the case of pyr_2C_x with $x > 2$ and 1.25 units for pyr_2C_2. These values show that although coordination of the first Ag^+ ion to the pyr_2C_x molecule is less favoured than protonation, the coordination of a second metal ion to LAg^+ is more favoured than addition of a second proton to HL^+. These findings indicate that the electrostatic repulsions between two Ag^+ ions coordinated to pyr_2C_x are less important than those between two protons linked to the same molecule, the effect being specially important for the case of pyr_2C_2.

The comparison between the values of $\log K_{H2}$ and $\log K_{H-Ag}$ (Table 3) shows that although formation of LAg^+ is less thermodynamically favoured than formation of HL^+, coordination of an Ag^+ ion to the HL^+ species is more favoured than the addition of a second proton. A similar conclusion is obtained by comparing the $\log K_{Ag-H}$ values with $\log K_{Ag2}$ or $\log K_{H2}$, which indicates that there is also a certain degree of cooperativity in the binding of a Ag^+ ion and a proton to a molecule of pyr_2C_x that results in the stabilisation of the $HLAg^{2+}$ species.

The cooperative effect observed for the addition of a proton and, to a lower extent, a second Ag^+ ion to the LAg^+ species can be also explained by considering that the structure of the complexes in solution is similar to that found in the solid state for the $[Ag(pyr_2C_2)(NO_3)]_2$ **1** and $[Ag(Hpyr_2C_4)(NO_3)_2]_2$ **4**. In the absence of coordinated nitrates, a significant electrostatic repulsion is expected between LAg^+ and the H^+ or Ag^+ cations. However, coordination of the nitrates results in uncharged or negatively charged $[Ag(pyr)(NO_3)]_2$ or $[Ag(pyr)(NO_3)_2]_2^{2-}$ cores (pyr = one pyrimidine sub-unit of the pyr_2C_x ligand) that favour the binding of positively charged species as Ag^+ or H^+. Thus, the cooperative effect would not be associated to an interaction between the pyrimidine rings but to the electrostatic effects associated to coordination of the nitrate anions.

Conclusion

Polymethylene-bis(2-aminopyrimidines) are useful ligands to interact with Ag(I) yielding discrete metallocycles. The ability of these ligands to form Ag(I) complexes, both in solid state {$[LAg(NO_3)]_2$ (L = pyr_2C_2) and $[HLAg(NO_3)_2]_2$ (L = pyr_2C_4) complexes} and solution, has been demonstrated.

The presence of -$(CH_2)_x$-linkers in pyr_2C_x complexes yield non-planar $(H_yLAg)_2^{2+2y}$ structural units ($y = 0$, 1) where each single pyrimidine ring acts as a bridge between two metal centres. Each macrocycle moiety interacts with their surroundings through weak interactions, yielding 3D structures. This preliminary studies show that the size and structural characteristics of these cycles depend on the length of the linker, which are the first step to perform new metallocyles with improved characteristics.

Experimental

Analytical and physical measurements

Elemental analyses were carried out using Carlo-Erba models 1106 and 1108 and Thermo Finnigan Flash 1112 microanalysers. Infrared spectra (KBr pellets) were recorded on a Bruker IFS 66. ^{1}H and ^{13}C NMR spectra were obtained with a Bruker AMX 300 spectrometer. Proton and carbon chemical shifts in dimethyl sulfoxide solution (DMSO-d_6) were referenced to DMSO-d_6 itself [^{1}H NMR, δ(DMSO) = 2.50; ^{13}C NMR, δ(DMSO) = 39.5 ppm]. All organic and inorganic (Sigma and Aldrich) reagents were used without further purification. Thermogravimetric data in the temperature range from 30 to 700 °C were recorded in a flowing air atmosphere (heating rate 5 °C min^{-1}) on a TA Instruments SDT 2960 Simultaneous DSC-TGA thermobalance. Selected IR and NMR data are included in Table 1 and in Electronic Supplementary Information

Synthesis of the ligands and complexes

***N*,*N*′-Bis(2-pyrimidyl)-α,ω-polymethylenediamine [pyr_2C_x (x = 2–6)].** The preparation of the ligands was carried out by a modification of a method previously described in the literature.[6] A suspension of 2-chloropyrimidine (1.1 g, 9.6 mmol) in *n*-butanol (20 cm^3) and triethylamine (3 cm^3) were refluxed with the required amount of α,ω-polymethylenediamine (4.8 mmol) during 4 h. The resulting solids were filtered off and washed with cold water and cold acetone to remove the impurities of triethylammonium hydrochloride that contaminate the crude materials. Further purification can be achieved by recrystallisation from boiling water.

***N*,*N*′-Bis(2-pyrimidyl)-1,2-ethylenediamine (pyr_2C_2) I.** (65–70%) (Found: C, 55.49; H, 5.73; N, 38.80%. Calc. for $C_{10}H_{12}N_6$: C, 55.54; H, 5.59; N, 38.86%); The corresponding $[(H\text{-}pyr)_2C_2](NO_3)_2$ compound **Ia** was obtained as a crystalline material (50% yield) by slow evaporation of the ligand dissolved in 0.1 M HNO_3.

***N*,*N*′-Bis(2-pyrimidyl)-1,3-trimethylenediamine dihydrate ($pyr_2C_3 \cdot 2H_2O$) II.** 35–60%). The large changes in the yield obtained in different preparations of this compound can be related to its higher solubility both in the water and the acetone washing fractions. The resulting compound exhibits a mass decrease (Found 13.40; Calc. 13.53) in the TG between 30 and 95° that corresponds to the loss of two water molecules per formula unit (Found: C, 49.93; H, 6.87; N, 31.66%. Calc. for $C_{11}H_{18}N_6O_2$: C, 49.61; H, 6.81; N, 31.56%).

***N*,*N*′-Bis(2-pyrimidyl)-1,4-tetramethylenediamine (pyr_2C_4) III.** (65–70%) (Found: C, 58.85; H, 6.88; N, 34.17%. Calc. for $C_{12}H_{16}N_6$: C, 59.00; H, 6.60; N, 34.40%); The corresponding $[(H\text{-}pyr)_2C_4](NO_3)_2$ compound (**IIIa**) was obtained as a crystalline material (80% yield) by slow evaporation of the ligand dissolved in 0.1 M HNO_3.

***N*,*N*′-Bis(2-pyrimidyl)-1,5-pentamethylenediamine (pyr_2C_5) IV.** (60–65%) (Found: C, 60.43; H, 7.11; N, 32.28%. Calc. for $C_{13}H_{18}N_6$: C, 60.44; H, 7.02; N, 32.53%).

***N*,*N*′-Bis(2-pyrimidyl)-1,6-hexamethylenediamine (pyr_2C_6) V.** (60–65%) (Found: C, 61.69; H, 7.51; N, 30.86%. Calc. for $C_{14}H_{20}N_6$: C, 61.74; H, 7.40; N, 30.86%).

2-(Butylamino)pyrimidine (pyrBu) VI.[12]. A suspension of 2-chloropyrimidine (1.1 g, 9.6 mmol) in *n*-butanol (20 cm^3) and triethylamine (3 cm^3) were refluxed with *n*-butylamine (0.7 g, 9.6 mmol) during 4 h and then allowed to stand at room temperature. The resulting crystalline solid (triethylammonium hydrochloride) was filtered off and washed with acetone. The *n*-butanol and acetone solutions were mixed and evaporated in vacuum, yielding a syrup that was treated with concentrated ammonium hydroxide and evaporated again, 2-(butylamino)pyrimidine was then obtained as an oily product (80%).

Preparation of Ag(I) complexes

The general procedure for the preparation of the Ag(I) complexes is as follows: the corresponding pyr_2C_x ligand (0.5 mmol) were dissolved in 0.05 M HNO_3 (20 cm^3) and an approximately fourfold excess of $AgNO_3$ (*ca* 1.75 mmol) were added. The resulting solution was refluxed during 1 h and after that time, the solution was filtered off and stored in darkness. If relevant, specific details for the different compounds are given below.

$[Ag(pyr_2C_2)(NO_3)]_2$ 1. Following the general procedure, slightly yellow crystals (50–60% yield) of composition $pyr_2C_2 \cdot AgNO_3$ and suitable for X-ray crystallography were obtained after several days (3–7 days). The results of the X-ray diffraction studies indicate that the complex is better formulated as $[Ag(pyr_2C_2)(NO_3)]_2$. Thermal gravimetric analysis (TGA) shows the presence of one Ag(I) per formula unit (Found 26.98; Calc. 26.96) (Found: C, 31.29; H, 3.14; N, 25.54%. Calc. for $C_{10}H_{12}AgN_7O_3$: C, 31.11; H, 3.13; N, 25.39%).

$pyr_2C_3 \cdot AgNO_3$ 2. Following the general procedure, after cooling the solution at room temperature, a white precipitate corresponding to a composition $pyr_2C_3 \cdot AgNO_3$ was obtained (10% yield). Although no crystals suitable for X-ray analysis could be obtained, a formula $[Ag(pyr_2C_3)(NO_3)]_2$ can be tentatively proposed by analogy with the corresponding pyr_2C_2 complex (Found: C, 33.12; H, 3.40; N, 24.43%. Calc. for $C_{11}H_{14}AgN_7O_3$: C, 33,02; H, 3,53; N, 24,50%). The $pyr_2C_3 \cdot AgNO_3$ complex can be obtained in an improved yield (*ca*. 80%) by reaction between the bis-pyrimidine ligand and $AgNO_3$ in water during 60 min.

$pyr_2C_4 \cdot AgNO_3$ 3 and $[Ag(Hpyr_2C_4)(NO_3)_2]_2$ 4. The general procedure leads first to a microcrystalline material (*ca* 30% yield) corresponding to a composition $pyr_2C_4 \cdot AgNO_3$ **3** (Found: C, 34.82; H, 3.82; N, 23.44%. Calc. for $C_{12}H_{16}AgN_7O_3$: C, 34.80; H, 3.89; N, 23.67%). On the other hand, it can be obtained in an improved yield (*ca* 80%) by reaction between the bis-pyrimidine ligand and $AgNO_3$ in water during 60 min. Although no crystals suitable for X-ray analysis could be obtained, a formula $[Ag(pyr_2C_4)(NO_3)]_2$ can be also tentatively proposed by analogy with the corresponding pyr_2C_2 complex.

After isolation of $pyr_2C_4 \cdot AgNO_3$ by the general synthetic route, a last fraction of slightly brownish hygroscopic crystals of composition $pyr_2C_4 \cdot AgNO_3 \cdot 2HNO_3$ **4** and suitable for X-ray crystallography was obtained after several weeks (*ca*. 20% yield). The results of the X-ray studies indicate that the complex must be formulated as $[Ag(Hpyr_2C_4)(NO_3)_2]_2$. Thermal Gravimetric analysis (TGA) shows one Ag(I) per formula unit (Found 19.1; Calc. 22.6) (Found: C, 29.61; H, 3.36; N, 22.93%. Calc. for $C_{12}H_{17}AgN_8O_6$: C, 30.20; H, 3.59; N, 23.48%).

Equilibrium measurements

The equilibrium constants for protonation of the ligands (pyr_2C_x compounds) and for the formation of the Ag(I) complexes were obtained from the analysis of potentiometric titrations carried out at 25.0 ± 0.1 °C under a N_2 atmosphere in the presence of 0.10 M KNO_3 as supporting electrolyte. Stock solutions of KOH and HNO_3 were prepared at concentrations close to 0.10 M; the KOH solution was titrated with potassium hydrogen phthalate

Table 4 Crystallographic data of ligands **Ia**, **IIIa**, and **IV**[a]

	$pyr_2C_2 \cdot 2HNO_3$ **Ia**	$pyr_2C_4 \cdot 2HNO_3$ **IIIa**	pyr_2C_5 **IV**
Formula	$C_{10}H_{14}N_8O_6$	$C_{12}H_{18}N_8O_6$	$C_{13}H_{18}N_6$
M_r	342.29	370.34	258.33
Crystal system	Monoclinic	Triclinic	Orthorhombic
Space group	$C2/c$	$P\bar{1}$	$Pcab$
a/Å	19.812(2)	4.8927(7)	8.4387(12)
b/Å	6.892(10)	7.4395(14)	17.711(3)
c/Å	11.955(2)	12.6052(15)	18.242(4)
α/°		107.169(14)	
β/°	114.135(12)	90.492(11)	
γ/°		108.333(14)	
V/Å^3	1490(2)	413.51(11)	2726.5(8)
Z	4	1	8
D_c/Mg m^{-3}	1.526	1.487	1.259
μ/mm^{-1}	0.128	0.121	0.082
Crystal size/mm	0.53 × 0.21 × 0.17	0.56 × 0.36 × 0.34	0.65 × 0.20 × 0.20
Data/restraints/parameters	2173/0/109	2404/0/118	2747/0/172
Final $R1$, $wR2$ [$I > 2\sigma(I)$]	0.0647, 0.1788	0.0523, 0.1492	0.0423, 0.1103
R Indices (all data)	0.1040, 0.2081	0.0705, 0.1652	0.1363, 0.1372

[a] Details in common T/K = 294(2).

Table 5 Crystallographic data of Ag(I) complexes **1** and **4**[a]

	$[Ag(pyr_2C_2)(NO_3)]_2$ **1**	$[Ag(Hpyr_2C_4)(NO_3)_2]_2$ **4**
Formula	$C_{10}H_{12}AgN_7O_3$	$C_{24}H_{34}Ag_2N_{16}O_{12}$
M_r	386.14	954.41
Crystal system	Triclinic	Triclinic
Space group	$P\bar{1}$	$P\bar{1}$
a/Å	8.930(6)	7.878(7)
b/Å	9.214(3)	9.067(5)
c/Å	9.765(9)	13.252(9)
α/°	71.40(3)	73.53(5)
β/°	84.08(4)	84.45(4)
γ/°	62.20(4)	70.23(4)
V/Å^3	672.7(7)	854.2(11)
Z	1.906	1.185
D_c/Mg m^{-3}	1	1
μ/mm^{-1}	1.521	1.232
Crystal size/mm	0.45 × 0.36 × 0.24	0.60 × 0.30 × 0.30
Data/restraints/parameters	3911/0/191	3016/0/248
Final $R1$, $wR2$ [$I > 2\sigma(I)$]	0.0356, 0.0980	0.0356, 0.0970
R Indices (all data)	0.0368, 0.0988	0.0387, 0.0987

[a] Details in common T/K = 294(2).

(phenolphthalein indicator) and was then used to titrate the HNO_3 solution with the same indicator. The Ag(I) solution used in the titrations was a standardized (0.1040 M) $AgNO_3$ solution obtained from Aldrich. The titrations were carried out with a Crison 2002 pH-meter provided with an Ingold combined electrode and calibrated to read pH as $-\log [H^+]$ by fitting the data corresponding to titrations of the HNO_3 solution with KOH. For each titration used to derive stability constants, a solution of the corresponding pyr_2C_x (L) ligand (40.0 cm^3) with a concentration close to 1.0×10^{-3} M was prepared in water containing the supporting electrolyte, and then the required amounts of the HNO_3 and $AgNO_3$ solutions were added before titration with KOH. The pyr_2C_6 ligand could not be studied because of solubility problems. The titrations of solutions containing Ag(I) were carried out in the dark, which hinders the observation of the reaction mixture to check the possible formation of precipitate. For this reason, the titrations were stopped when the pH readings became erratic or the titration curve showed any discontinuity. This occurred typically at pH close to 5–6, and observation of the reaction mixture at this point confirmed in all cases the formation of precipitate. Titrations of the ligands in the absence of Ag(I) also showed precipitation at the same pH values. Thus, the pH range covered in the potentiometric studies is *ca.* 2.5–5.5, with small changes for each particular titration. A total of 20–50 points were measured during each titration and the data were analysed with the program HYPERQUAD.[13]

The protonation constants of the ligands were obtained from two titrations of the ligand alone, and the equilibrium constants for the formation of Ag(I)–L complexes were then obtained from titration of solutions containing Ag(I) and L in 2 : 1 and 1 : 1 molar ratios. Attempts to carry out titrations with a larger Ag(I) : L molar ratio were unsuccessful because precipitation occurs at pH values too low to permit the derivation of equilibrium constants. For titrations in the presence of the metal ion, the formation constants corresponding to the protonated forms of the ligand were fixed at the values derived from titrations of the ligand alone. During all refinements the value of $\log K_w$ was fixed at -13.78 and the Ag(I)–OH^- complexes were also introduced in the model with formation constants fixed at their corresponding literature values,[14] although their effect is negligible because they are not formed at significant extent at the pH range covered in the present study.

Crystallographic studies

X-Ray data for single crystals of **Ia**, **IIIa**, **IV**, **1** and **4** were collected with an Enraf-Nonius CAD4 diffractometer, at 293(2) K, using monochromatic Mo-Kα radiation ($\lambda = 0.71069$ Å). The cell parameters were determined from a least-squares refinement against a set of reflections randomly searched. Data were collected at room temperature using ω–2θ scans. Lorentz-polarisation correction was applied using the WinGX program.[15] Absorption was corrected using psi-scans[16] (**IIIa**, **IV**) and DIFABS[17] (**Ia**, **1** and **4**). The structures were solved by direct methods [SHELX97 programs[18] (for **Ia**, **IIIa**, **IV** and **4**) and SIR2002 (for **1**)[19]] and refined by a full-matrix, least squares method.[18] **Ia** and **IIIa** bipyrimidine molecules lie on crystallographic symmetry elements, twofold for **Ia** and a center of symmetry of **IIIa**. Non-H atoms were anisotropically refined. In general, H atoms were positioned in calculated positions and their isotropic thermal vibration was fixed to 1.2–1.5 times the U_{iso} of the bonded atom. The H atom bonded to a nitrogen in the terminal ring in **4** was localized in Fourier difference maps in order to know the exact protonation site, N(1′) or N(3′). Moreover, its isotropic thermal vibration parameter was also refined. Crystal parameters, data collection details and results of the refinements are summarized in Tables 4 and 5.

CCDC reference numbers 273769 (**Ia**), 273770 (**IIIa**), 273771 (**IV**), 273722 (**1**) and 273773 (**4**).

See http://dx.doi.org/10.1039/b508260a for crystallographic data in CIF or other electronic format.

Acknowledgements

We are grateful to the Spanish CICYT (BQ2002-02546 and BQ2003-04737) and to the Junta de Andalucía (FQM-135) for financial support. We also provide thanks for the COST D20 (WG 0006) project

References

1 J. M. Lehn, in *Supramolecular Chemistry-Concepts and Perspectives*, VCH, Weinheim, 1995.
2 (*a*) R.-H. Wang, M.-C. Hong, W.-P. Su, Y.-C. Liang, R. Cao, Y.-J. Zhao and J.-B. Weng, *Inorg. Chim. Acta*, 2001, **323**, 139–146; (*b*) C. V. K. Sharma, S. T. Griffin and R. D. Rogers, *Chem. Commun.*, 1998, 215–216; (*c*) C. V. K. Sharma and R. D. Rogers, *Cryst. Eng.*, 1998, **1**, 19–38.
3 J. A. R. Navarro, J. M. Salas, M. A. Romero and R. Faure, *J. Chem. Soc., Dalton Trans.*, 1998, 901–904.
4 H. Cai, H.-M. Hu, W.-Z. Chen, H.-G. Zhu and X.-Z. You, *Chem. Lett.*, 1999, 221–222.
5 P. O. Lumme and H. Knuuttila, *Polyhedron*, 1995, **14**, 1553–1563.
6 A. García-Raso, J. J. Fiol, F. Bádenas, A. Tasada, X. Solans, M. Font-Bardia, M. G. Basallote, M. A. Máñez, M. J. Fernández-Trujillo and D. Sánchez, *J. Inorg. Biochem.*, 2003, **93**, 141–151.
7 G. R. Desiraju and T. Steiner, in *The Weak Hydrogen Bond*, International Union of Crystallography, Oxford Science, Oxford, 1999, ch. 2.
8 J. Kulig, B. Lenarcik and M. Rzepka, *Pol. J. Chem.*, 1986, **60**, 715–724.
9 L. N. Balyatinskaya and Y. F. Milyaev, *Koord. Khim.*, 1976, **2**, 1594–1599.
10 G. Berthon and O. Enea, *Thermochim. Acta*, 1973, **6**, 57–65.
11 H. L. Zhu, S. Yang, J. L. Ma, X. Y. Qiu, L. Sun and S. C. Shao, *Acta Crystallogr., Sect. E*, 2003, **59**, m1046–m1047.
12 I. C. Kogon, *J. Org. Chem.*, 1956, **21**, 1027–1028.
13 P. Gans, A. Sabatini and A. Vacca, *Talanta*, 1996, **43**, 1739–1753.
14 A. Guebeli and J. Ste-Marie, *Can. J. Chem.*, 1967, **45**, 827–832.
15 L. J. Farrugia, *J. Appl. Crystallogr*, 1999, **32**, 837–838.
16 A. C. T. North, D. C. Phillips and F. S. Mathews, *Acta Crystallogr., Sect. A*, 1968, **24**, 351–359.
17 N. Walker and D. Stuart, *Acta Crystallogr., Sect. A.*, 1983, **39**, 158–166.
18 G. M. Sheldrick, *SHELX-97, A Program for Crystal Structure Analysis (Release 97-2)*, University of Göttingen, Germany, 1997.
19 M. C. Burla, M. Camalli, B. Carrozzini, G. L. Cascarano, C. Giacovazzo, G. Polidori and R. Spagna, Sir2002: a new Direct Methods program for automatic solution and refinement of crystal structures, *J. Appl. Crystallogr.*, 2003, **36**, 1203.